IEEE Transactions on Nuclear Science, Vol. NS-28, No. 3, June 1981

INTENSE LOW-EMITTANCE-ELECTRON-GUN DEVELOPMENT AT PHERMEX*

J. C. Elliott, R. J. Faehl, H. J. Fullbright, D. C. Moir, and C. E. Swannack
Los Alamos National Laboratory, Los Alamos, NM 87545

Introduction

The PHERMEX facility consists of a 50-MHz standing-wave linear accelerator. Electrons with up to 550-keV kinetic energy are injected into the accelerating column by a hot-cathode electron gun. The present 100-mm-diam cathode has been in operation since 1963.[1] The gun has performed extremely well since that time, and to date there have been no substantial design changes. Early gun experiments involved measurement of current, voltage, and beam distribution; however, no emittance measurements had been made. As part of the PHERMEX upgrade program, it was felt that this gun design could be extended to higher perveance. Early experiments indicated that it was necessary to maintain beam quality to transport the beam through the three PHERMEX accelerator cavities.

Experimental Results

Details of the electron-gun design, materials, and engineering are described extensively in Ref. 1. Here we discuss only the anode-cathode (A-K) geometry as it relates to our experiments. Figure 1 is a drawing of the PHERMEX standard 100-mm gun A-K geometry.

A type-B dispenser cathode operated at 1100°C was selected as the best possible cathode for PHERMEX application. It has a long lifetime and is not extremely susceptible to poisoning. All of the experiments discussed in this paper have used this type cathode.

Figure 2 is a schematic diagram of the experimental arrangement. The voltage is supplied across the A-K gap by a 600-kV Femcor pulser. The pulser is a Marx generator with coaxial-cable capacitor elements. The internal impedance of the pulser is 280 Ω and is matched by placing a load resistor in parallel with the electron gun. The pulser voltage is monitored by measuring the voltage across a low resistance (0.1 Ω) in series with the load resistor. Figure 3a shows a typical voltage trace measured across the current-viewing resistor (CVR).

Current to the gun is measured using a Pearson Model 410 current monitor. The monitor signal is converted to light by a light-emitting current diode. The light is transmitted through an optical fiber to a light-to-voltage converter, and the signal is monitored by an oscilloscope. At present, this monitor has a bandwidth of 10-to-50 MHz. Development of a faster monitor is in progress. Figure 3b is the signal measured by this monitor.

The hot cathode is pulsed with a negative voltage and electrons are driven through the anode aperture. The resulting cylindrical electron beam strikes a 1.5-mm-thick, 102-mm-diam disk. The disk contains a cylindrically symmetric hole pattern with slots for determining the beam diameter. Figure 4 is a diagram of this disk. Approximately 98% of the beam is intercepted by the disk. The collected electron current on the disk goes to ground through twenty 10-Ω, 2-W carbon resistors in parallel. This resistance was measured to be 0.510 Ω. The voltage across the resistor ring was monitored and a sample trace is shown in Fig. 3c. This was used for the time-resolved current measurement.

The beamlets, which are transmitted through the aluminum mask, drift 102 mm and impinge on an aluminized glass surface. Light is generated by the electron-aluminum oxide interaction and is transmitted through the glass. Photographs are taken of the beamlet distribution. A typical photograph is shown in Fig. 5.

Three experiments involving minor design changes in the A-K geometry will be discussed in detail. These include: (1) standard gun A-K geometry (Fig. 1 solid line); (2) standard gun with return-current cone (Fig. 1 solid line plus copper return-current cone noted by the dashed line); and (3) same as (2) with the A-K gap, d, decreased by 5.1 mm.

Data

Figures 3a and 3c are typical current-viewing resistor and emittance-mask/charge-collector voltage traces, respectively. The CVR gives a measure of the voltage on the gun because all elements shown in Fig. 2 schematic are in parallel. The charge collector yields a proportional measurement of the beam current extracted from the cathode. The current and voltage are measured at the 150-ns width of the pulse. Results of these measurements for all three experiments are shown in Columns 2 and 3 of Table I. The gun perveance, g, is calculated from the formula

$$I = gV^{3/2}$$

and is shown in Column 4.

The beam emittance is determined from the beamlets distribution shown in Fig. 5. The negatives of the photographs are scanned with a microdensitometer. Each film is processed with a step wedge to verify that the photographic data are in a linear response range of the film. Figure 6 shows a microdensitometer scan using a 25-μm aperture. It should be noted that the background is flat. Line scans at various azimuthal angles have indicated cylindrical symmetry. The densitometer data are analyzed similar to the technique outlined in Ref. 2. The only difference is that the FWHM of each beamlet is used in determining the value of its angular dispersion $d\alpha$. In Ref. 2, the beamlet width is measured at the average beam half-maximum. Therefore, the technique of Ref. 2 yields an emittance which is weighted by the beam distribution. To the extent that the PHERMEX electron-gun beam distribution is flat, the techniques are identical. Figure 7 is a plot of the beam distribution for various voltages as obtained from microdensitometer scans. These results indicate that the aluminum oxide is a linear detector, i.e., the integrals of the distributions that are connected for film response and energy loss follow the $V^{3/2}$ law. The emittance at a voltage is calculated and given in Column 5 of Table I. A sample r vs α plot from which the emittance is determined is shown in Fig. 8.

Experimental Arrangements

The electron-gun perveance depends only on the A-K geometry. Therefore, the internal consistency of the perveance calculation for a single experiment is a measure of the relative accuracy of the technique used to determine the voltage and current. The average value of the perveance for each experiment is summarized in Table II. It should be noted, however, that the absolute measure of the perveance probably contains systematic errors. Here we desire only internal consistency for intercomparison. A measure of the internal constancy is presented by the statistical error quoted in Table II.

Clearly, the addition of the return-current cone (Exp. 2) did not change the perveance. However, displacement of the anode 5.1 mm toward the cathode (Exp.

*Work performed under the auspices of the U.S. Department of Energy.

3) did increase the perveance by 15%.

A substantial improvement in emittance was realized simply by the addition of the return-current cone. Apparently the presence of a transverse gap just beyond the anode of the standard gun configuration induces a significant amount of transverse momentum in the beam through lack of local image currents flowing near the beam axis in the region just beyond the anode. Displacement of the anode toward the cathode (Exp. 3) increases the beam area at emittance mask substantially (30%). However, the presence of the return-current shield decreases the emittance and makes it comparable to that of standard gun configuration at the same voltage.

Theoretical Results

The time-dependent, two-dimensional Particle-in-Cell (PIC) simulation code CCUBE has been used to study beam dynamics in the A-K gap. Although the code has been successfully used on a variety of intense beam problems, initial studies were directed at code validation for the existing standard gun geometry. Such numerical tools include all self-consistent fields but at the expense of limited resolution and enhanced high-frequency noise. Since perveance is determined by the geometry for space-charge-limited flow, this parameter was felt to provide a fair test of resolution. Perveance of the calculated beams was found to agree with experiment to within 10-20%. Though the values were consistently lower than experimental ones, scaling was consistent. Numerical values for voltage of 450 kV are given in Table II. Further, inclusion of a conducting shield beyond the anode aperture seemed to reduce the transverse energy of the transported beam. Future calculations will quantify the emittance. Finally, a trial variation on the standard gun geometry has resulted in an increase of calculated perveance from 0.8 μperv to 1.8 μperv at 1.022 MV.

Conclusions

Experimental measurements and theoretical calculations have been performed and compared for the PHERMEX standard electron gun. Slight changes in the gun configuration have produced significant changes in beam intensity and quality. It is hoped that the present gun configuration can be extended to even higher perveances (without significant loss of beam quality) through a joint theoretical and experimental effort.

REFERENCES

1. Venable, D., et al, "PHERMEX: A Pulsed High-Energy Radiographic Machine Emitting X-Rays," Los Alamos National Laboratory report LA-3241 (May 1967).

2. Kulke, B. and Kihara, R., "Emittance Measurement on Field Emitter Diodes, Proceedings of 2nd International Pulse Power Conference, 209 (1979).

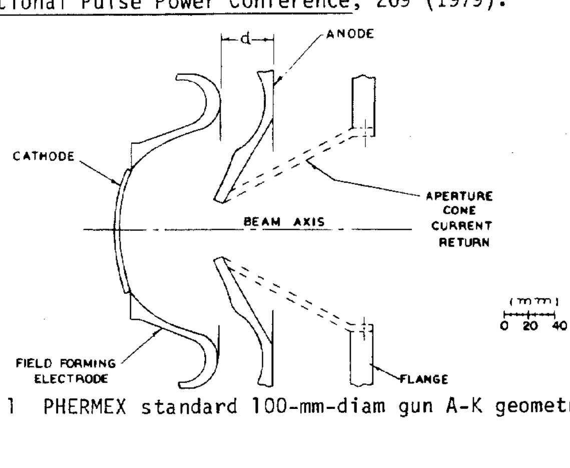

Fig. 1 PHERMEX standard 100-mm-diam gun A-K geometry

TABLE I

UNNORMALIZED EMITTANCE

Experiment Number	V(kV)	I(A)	g(μP)	$\frac{\epsilon}{\pi}$(mm-mrad)
1	268	122	0.89	-
	350	196	0.95	-
	438	279	0.96	102
2	269	122	0.87	-
	352	185	0.89	-
	425	263	0.95	-
	466	292	0.91	88
3	254	136	1.06	-
	338	208	1.06	-
	364	230	1.05	-
	396	274	1.10	-
	434	311	1.09	-
	452	329	1.08	96

TABLE II

EXPERIMENTAL GUN PERVEANCES

Experiment Number	g_{ave}(μP)	g_{thry}(μP)
1	0.93 ± 0.04	0.80 ± 0.01
2	0.90 ± 0.04	0.80 ± 0.01
3	1.07 ± 0.02	0.97 ± 0.01

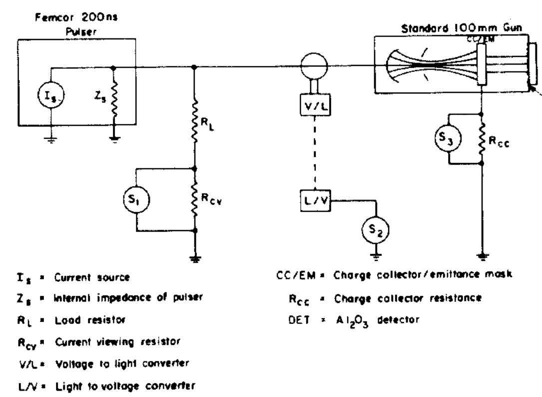

Fig. 2 Schematic electron-gun experimental arrangement

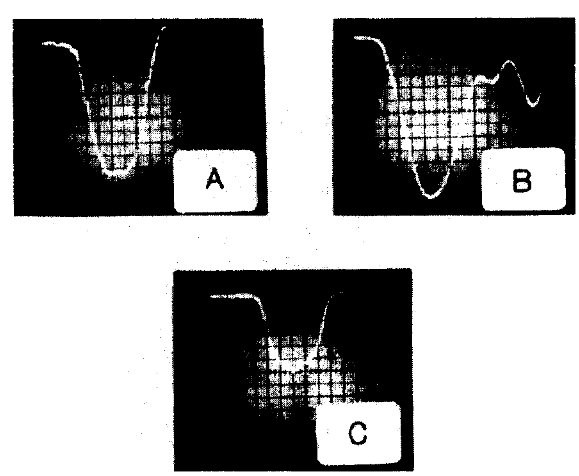

Fig. 3 Measurements of the gun (a) voltage, (b) current to the gun, and (c) transmitted current (all 100 ns/div)

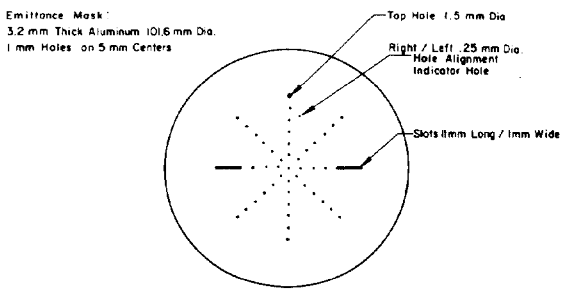

Fig. 4 Emittance-mask charge collector

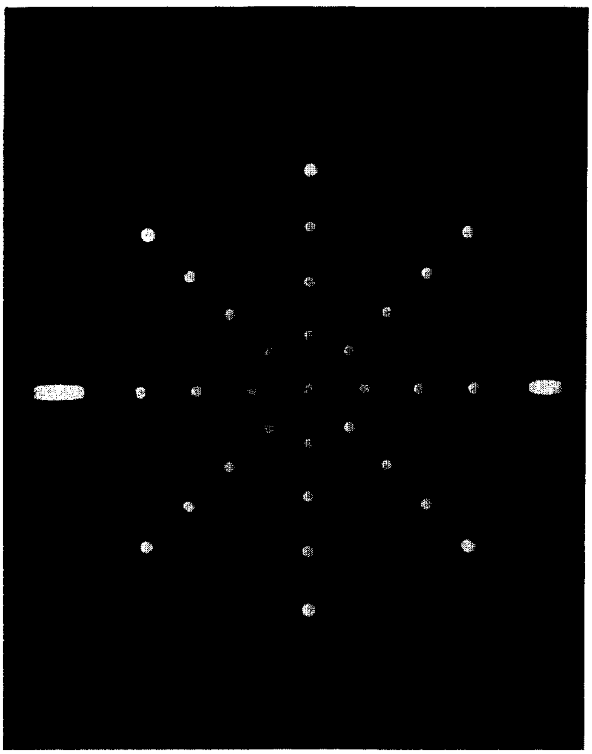

Fig. 5 Typical emittance record using slotted mask

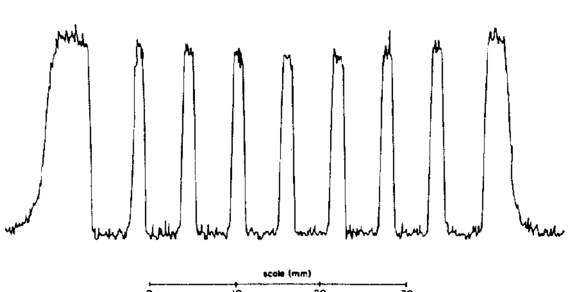

Fig. 6 Microdensitometer trace of an emittance record

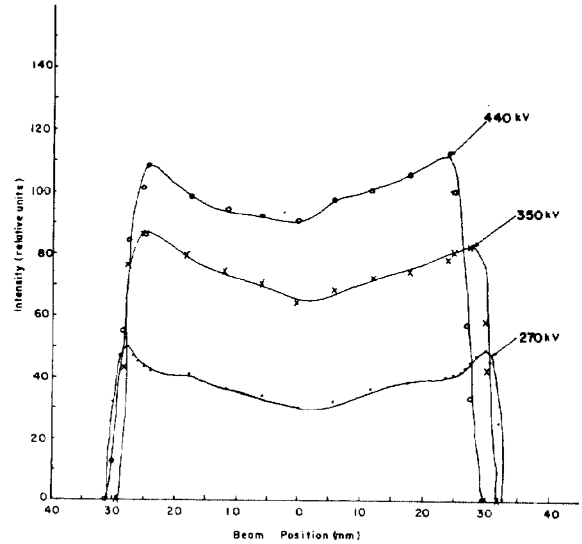

Fig. 7 Intensity distribution, standard gun

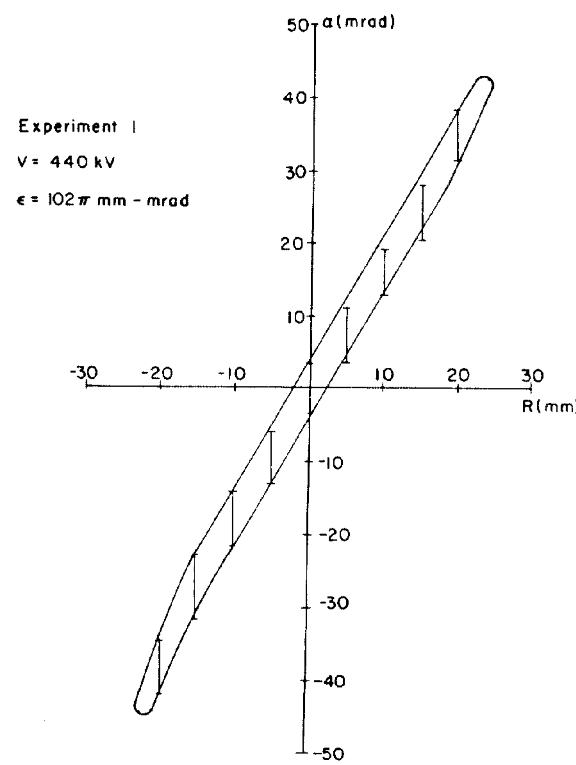

Fig. 8 Emittance plot for standard 100-mm-diam electron gun